

UNCLASSIFIED

Defense Technical Information Center
Compilation Part Notice

ADP012244

TITLE: Magic Family of Discretely Sized Ultrabright Si Nanoparticles

DISTRIBUTION: Approved for public release, distribution unlimited

This paper is part of the following report:

TITLE: Nanophase and Nanocomposite Materials IV held in Boston, Massachusetts on November 26-29, 2001

To order the complete compilation report, use: ADA401575

The component part is provided here to allow users access to individually authored sections of proceedings, annals, symposia, etc. However, the component should be considered within the context of the overall compilation report and not as a stand-alone technical report.

The following component part numbers comprise the compilation report:

ADP012174 thru ADP012259

UNCLASSIFIED

MAGIC FAMILY OF DISCRETELY SIZED ULTRABRIGHT SI NANOPARTICLES

G. BELOMOIN, J. THERRIEN, A. SMITH, S. RAO, R. TWESTEN, S. CHAIEB^{b)}, AND M. H. NAYFEH

Department of Physics and Department of Theoretical and Applied Mechanics^{b)}, University of Illinois at Urbana-Champaign, 1110 W. Green Street, Urbana, Illinois 61801 USA

L. WAGNER, AND L. MITAS

Department of Physics, North Carolina State University, 127 Stinson Rd., Raleigh, NC 27695

ABSTRACT

We describe a procedure for dispersion bulk Si into a family discretely sized ultrasmall ultrabright nanoparticles. We demonstrate that electrochemically etched, hydrogen capped Si_nH_x clusters with n larger than 20 are obtained within a family of discrete sizes. These sizes are 1.0 (Si_{29}), 1.67 (Si_{123}), 2.15, 2.9, and 3.7 nm diameter. We characterize the particles via direct electron imaging, excitation and emission optical spectroscopy, chromatography, and colloidal crystallization. The band gaps and emission bands are measured. The smallest four are ultrabright blue, green, yellow, and red luminescent particles. The availability of discrete sizes and distinct emission in the red, green and blue range is useful for biomedical tagging, RGB displays, and flash memories.

INTRODUCTION

Semiconductor clusters, especially silicon clusters, is currently one of the most active frontiers in physics and chemistry [1-20]. Their unique structures, stability, and optical and electronic and chemical reactivity, both in free space and on surface have been examined [3]. Fabricating size-, shape-, and orientation-controlled fluorescent Si nanoparticles in the range 1-3 nm (30-1000 atoms), with reproducibility would be critical to the understanding of nanostructures and would be of significant interest to the microelectronics, optoelectronics and biomedical industries. Averaging over size or shape inhomogeneously masks spectroscopic properties, hindering testing of theory. Size uniformity is important for applications that require superlattices, high quality films, or single nanoparticle-based devices, such as fluorescent imaging and tagging. The availability of discrete sizes with distinct emission in the red, green and blue range is useful for biomedical tagging and in RGB display applications. In flash memory, nanoparticles are embedded in a MOSFET as floating gates to store electric charge. Since the shift in the device's threshold depends on the particle size, a wide size distribution would wash the operating threshold. Several efforts have been directed to develop procedures to control the size, and shape of Si nanoparticles. Only recently progress towards control over the crystallography orientation has been achieved [12].

Self-terminated clusters Si_n [6-8] with $n < 10$ exhibit discrete magic numbers, whereas the abundance spectrum of clusters Si_n with $n > 20$ exhibits neither special features nor discrete magic numbers [9]. The shape of those large ones, however, changes from prolate to more spherical in the narrow range between $n = 24$ and $n = 30$ [10]. In the prolate regime, atoms are arranged in one-shell and form triangular surface facets, while in the spherical regime, atoms are arranged into two shells. The outer one has the topology of a fullerene cage, and the inner

shell has a high coordination number. The bonds to the inner shell saturate most of the dangling bonds of the outer shell. The dissociation energy, which is a strongly size dependent for smaller clusters, is a smooth function of n for $n > 25$ [11].

Hydrogen-capped Si clusters Si_nH_x with H terminating the unsaturated bonds present opportunities to magic cluster research. Stable configurations with H capping have been recently presented [4-5]. Moreover, in some recent electrochemical etching measurements, hydrogen-capped Si in the 1-3 nm size regime has been shown to become highly fluorescent, exceeding the brightness of dyes such as fluorescein [13], and exhibits stimulated emission [14-15] and harmonic generation [16]. We recently demonstrated that, unlike uncapped Si_n particles, hydrogen-capped Si_nH_x particles ($n > 20$) exhibit magic discrete numbers [17]. We dispersed crystalline Si into H-terminated Si nanoparticles and used direct electron imaging, excitation and emission spectroscopy for characterization, and colloid crystallization for segregation. Transmission electron microscopy (TEM) shows that they classify into a family of discrete sizes that includes 1.0, 1.67, 2.15, 2.9, and 3.7 ± 0.1 nm diameter. Excitation spectroscopy measures for the four smallest a HUMO-LUMO gap of 3.44, 2.64, 2.39, and 2.11 eV, while emission spectroscopy shows that they are ultrabright UV/blue, green, yellow, and red luminescent particles with band peaks at $\sim 410, 540, 570$, and 600 nm.

SYNTHESIS

We use highly catalyzed electrochemical etching in HF and H_2O_2 to disperse crystalline Si into ultrasmall nanoparticles [18, 11]. The wafer is laterally anodized while being advanced into the etchant slowly to produce a large meniscus-like area. Because HF is highly reactive with silicon oxide, H_2O_2 catalyzes the etching, producing smaller particles. Moreover, the oxidative nature of the peroxides produces high- chemical and electronic quality samples. The pulverized wafer is then transferred to an ultra sound bath for a brief treatment, under which the film crumbles into colloidal suspension of ultrasmall blue particles. Larger particles are less amenable to dispersion due to stronger interconnections. We use a post HF treatment to weaken those and then an ultra sound treatment to disperse the particles. We centrifuge the mix. The resulting residue contains the largest red particles, while the suspension contains the green/yellow particles. We re-dissolve the residue and sonificate it. The red emitting particles stay in suspension. The green particles may be separated by additional sonification/ and or the addition of a drop of HF. Commercial Gel permeation chromatography may be used to separate the particles further, if necessary, or to obtain additional accuracy in separation of the other particles. The particles are separated into several vials each contains particles of uniform size, with near 90-100 % efficiency.

ELECTRON IMAGING

We immersed a thin graphite grid in the colloid and imaged it by high-resolution TEM [19]. **Fig. 1 (Top)** shows that particles are nearly spherical and classify into a small number of sizes. These include 1.0 (see inset), 1.67, 2.15, 2.9, and 3.7 nm. **Fig. 1 (Bottom)** shows the atomic planes in close ups of the 1.67, 2.15, 2.9 and 3.7 nm particles.

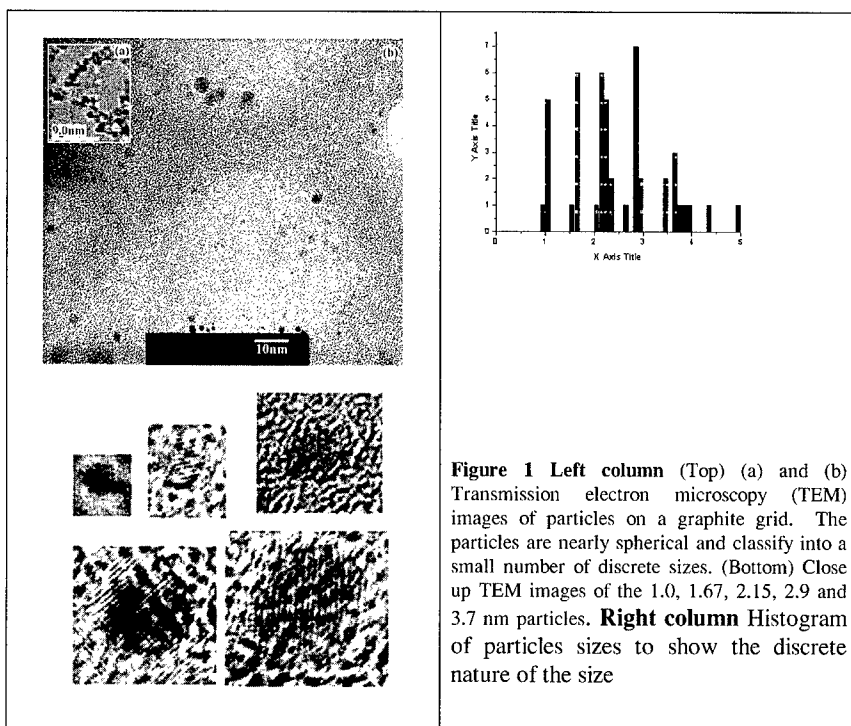


Figure 1 Left column (Top) (a) and (b) Transmission electron microscopy (TEM) images of particles on a graphite grid. The particles are nearly spherical and classify into a small number of discrete sizes. (Bottom) Close up TEM images of the 1.0, 1.67, 2.15, 2.9 and 3.7 nm particles. **Right column** Histogram of particles sizes to show the discrete nature of the size

OPTICAL CHARACTERIZATION OF MIXTURE

The absorption and emission gaps of the members of the family were examined. The excitation, i.e., the absorption monitored at a specific emission wavelength (product of absorption and emission) was recorded on a photon counting spectro-fluorometer with a Xe arc lamp light source and 4 nm bandpass excitation and emission monochrometers. We mapped out the excitation in the range 250 nm and 800 nm, while monitoring the emission in the range 400-700 nm. We used the mapping to identify the resonance excitation structure. **Figure 2**, which presents the excitation, shows a resonance structure at 3.44 ± 0.1 , 2.64, and 2.39, and 2.11 eV. This resonance structure produces emission bands with maxima at 410, 540, 570, and 600nm respectively. We associate the resonance energies with the HUMO-LUMO edge E_g . According to quantum confinement, the absorption and emission photon energies correlate with the size. We pair the diameter d (in nm) with excitation resonance E_g (in eV) as follows (d, E_g): (1.0, 3.44); (1.67, 2.64); (2.15, 2.39); and (2.9, 2.11). However, we did not record an excitation/emission resonance that can be associated with the 3.7 nm diameter particle. This may be due to low abundance or/and diminished brightness. A power law fit gives $E_g = 3.44 / d^{0.5}$.

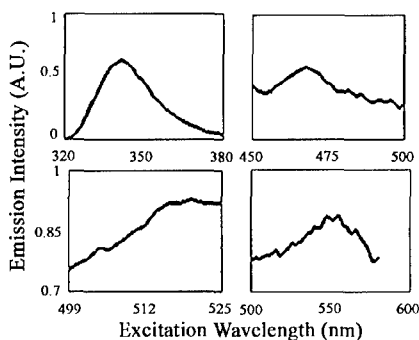


Figure 2 The excitation spectra of the 1.0, 1.67, 2.15, and 2.9 nm in diameter particles monitored at emission wavelengths 400, 540, 570, and 600nm respectively. They show local resonance structure at 3.44, 2.64, and 2.39, and 2.11 eV respectively.

PARTICLE SEGREGATION

Size uniformity is required for organization or self-assembly. Under certain conditions, the particles segregate according to size upon crystallization. Over time, 5 to 100 μm crystals have formed in a water colloid. Colloidal crystallites were placed on glass and illuminated with light from a mercury lamp (at 360, 395, 450, 520, 560, 610 nm). Emission is detected in the backward direction and detected by an RGB filter/prism based dispersive charge coupled device (3CCD). **Figure 3** (Top Row) shows examples of blue, green, and red segregated crystals. We associate those with the particles observed in the TEM images. Recrystallization to form yellow or green crystals takes place but they are less frequent compared to the blue and red. **Figure 3** (Bottom) gives a photo of colloids of the magic sizes under the irradiation from an incoherent low intensity commercial UV lamp at 365 nm, showing the characteristic red, yellow, green, blue colors.

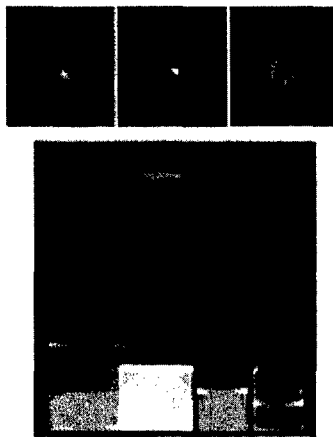


Figure 3 (Top row) The emission from blue, green, and red colloidal crystals segregated according to the magic sizes 1.0, 1.67, and 2.9 nm in diameter. The crystals are illuminated with light from a mercury lamp. The background is due to a weak bright field. (Bottom from right to left) The emission of colloids of members of the magic family of 1.0, 1.67, 2.15, and 2.9 nm in diameter, after they have been separated, under excitation using a commercial low intensity UV source with an average wavelength of 365 nm.

SIMULATION

We density functional with generalized gradient exchange-correlation potentials, Configuration Interaction and Monte Carlo approaches to construct structural prototype Si_nH_x particles and to calculate the HOMO-LUMO bandgap [5]. We start from a spherical piece of a crystalline Si. The dangling bonds are saturated with hydrogen. Pairs of H from adjacent surface Si atoms are stripped (by H_2O_2), and replaced by reconstructed Si-Si dimers, similar to the well-known Si (001) surface 2×1 reconstruction. Reconstructed Si-Si bonds have recently been proposed as a source of novel optical activity in ultrasmall particles [4,20]. The resulting structure was relaxed using the Density Functional Theory (DFT) with the PW91 exchange-correlation functional. The simulation yields stable sizes, including 1.0 nm ($\text{Si}_{29}\text{H}_{24}$) and 1.6 nm ($\text{Si}_{123}\text{H}_{xx}$), with band gaps of 3.5 and 2.67 eV respectively. **Figure 4** gives the prototype of the smallest (from ref 5). It is $\text{Si}_{29}\text{H}_{24}$ with five atoms constituting a tetrahedral core and 24 atoms constituting a H-terminated reconstructed Si surface. A single H atom terminates each surface Si atom. Earlier, Allan et al found that particles of 1.03 and 1.67 nm in diameters are stable with bandgaps of 3.5, and 2.67 eV, and consist of 29 and 123 Si atoms respectively [4].

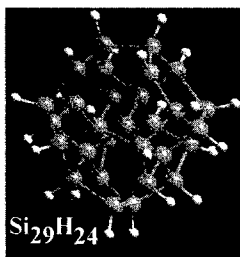


Figure 4 Prototype structures of $\text{Si}_{29}\text{H}_{24}$. In the particle, five Si atoms (dark sphere) constitute a single tetrahedral core and 24 Si atoms (dark sphere) constitute a H-terminated (white sphere) reconstructed surface.

The dependence of the bandgap on the number of terminating H atoms is interesting. We start from bulk-like Si_{29} cluster; 36 hydrogen atoms are needed to terminate the unsaturated bonds. As the number of H atoms is reduced from 36, the bandgap drops slowly. But for the number of hydrogen atoms below 24, the bandgap drops sharply, approaching a metallic zero bandgap, and requires bonding change from pure sp^3 tetrahedral diamond-like to a mix with sp^2 , a configuration common in carbon but does not exist in bulk Si. The particle is a filled fullurene of a highly puckered cage and belongs to TD magic structures.

CONCLUSION

We demonstrated that Si_nH_x clusters classify into a magic discrete family of spherical size that includes ~ 1.0 (Si_{29}), 1.67 (Si_{123}), 2.15, 2.9, and 3.7 nm diameter, emitting in the UV/blue, green, yellow, and red for the smallest four particles. So far we find no stable capped particles smaller than 29 atoms. We can predominantly produce 1 nm diameter blue particles, or 2.9 nm diameter red particles. Research will be conducted to refine conditions under which the green and yellow members of the family may be predominantly prepared.

ACKNOWLEDGMENT: We acknowledge the State of Illinois Grant IDCCA No. 00-49106, the US DOE Grant DEFG02-ER9645439, NIH Grant RR03155, and US NSF grant BES-0118053.

REFERENCES

1. Physics and Chemistry of Small Clusters, edited by P. Jena, B. Rao, and S. Khanna (Plenum, New York, 1987)
2. M. F. Jarold, *Science* **252**, 1085 (1981); K. M. Ho et al., *Nature (London)* **392**, 582 (1998); E. Kaxiras, and E. Jackson, *Phys. Rev. Lett.* **71**, 727 (1993); J. Grossman and L. Mitas, *Phys. Rev. Lett.* **74**, 1323 (1995); L. Mitas, J. Grossman, I. Stich, and J. Tobik, *Phys. Rev. Lett.* **84**, 1479 (2000); I. Vasiliev, S. Ogut, and J. Chelikowsky, *Phys. Rev. Lett.* **82**, 1919 (1999)
3. I-S. Hwang, M-S Ho, and T. T Tsong, *Phys. Rev. Lett.* **83**, 120 (1999)
4. G. Allan, C. Delerue, and M. Lannoo, *Phys. Rev. Lett.* **76**, 2961 (1996)
5. L. Mitas, J. Therrien, G. Belomoin, and M. H. Nayfeh, *Appl. Phys. Lett.* **78**, 1918 (2001)
6. W. Brown, R. Freeman, K. Raghavachar, and M. Schuller, *Science* **235**, 860 (1987); L. Bloomfield, R. Freeman, and W. Brown, *Phys. Rev. Lett.* **54**, 2246 (1985)
7. K. Raghavachari, *Phase Transitions* **24-26**, 61 (1990)
8. U. Rothlisberger, W. Andreoni, and M. Parrinello, *Phys. Rev. Lett.* **72**, 665 (1994); W. Andreoni, and G. Pastore, *Phys. Rev. B* **41**, 10243 (1990); U. Rothlisberger, W. Andreoni, and P. Giannozzi, *J. Chem Phys.* **96**, 1248 (1992)
9. L. Anderson, S. Muruyama, and R. Smalley, *Chem. Phys. Lett.* **176**, 348 (1991); H. Kroto, J. Heath, S. O'Brian, R. Curl, and R. Smalley, *Nature (London)* **318**, 162 (1985)
10. M. Jarrold, and V. Constant, *Phys. Rev. Lett.* **67**, 2994 (1991); M. Jarrold and J. Bower, *J. Chem. Phys.* **96**, 9180 (1992)
11. M. Jarrold and E. Honea, *J. Phys. Chem.* **95**, 9181 (1991)
12. G. Grom, D. Lockwood, J. McCaffrey, H. Labbe, P. Fauchet, B. White Jr., J. Dlenner, D. Kovalev, F. Koch, and L. Tsybeskov, *Nature* **407**, 358 (2000)
13. O. Akcikir, J. Therrien, G. Belomoin, N. Barry, E. Gratton, and M. Nayfeh *Appl. Phys. Lett.* **76**, 1857 (2000)
14. M. H. Nayfeh, N. Barry, J. Therrien, O. Akcikir, E. Gratton, and G. Belomoin, *Appl. Phys. Lett.* **78**, 1131 (2001); M. Nayfeh, O. Akcikir, J. Therrien, Z. Yamani, N. Barry, W. Yu, and E. Gratton, *Appl. Phys. Lett.* **75**, 4112 (1999)
15. M. H. Nayfeh, S. Chaieb, S. Rao, N. Barry, J. Therrien, G. Belomoin, and A. Smith, *Appl. Phys. Lett.* December 24 (2001)
16. M. H. Nayfeh, O. Akcikir, G. Belomoin, N. Barry, J. Therrien, and E. Gratton, *Appl. Phys. Lett.* **77**, 4086 (2000)
17. G. Belomoin, J. Therrien, A. Smith, S. Rao, R. Twisten, S. Chaieb, M.H. Nayfeh, L. Wagner, and L. Mitas, *Appl. Phys. Lett.* (In press)
18. Zain Yamani, Howard Thompson, Laila AbuHassan, and Munir H. Nayfeh *Appl. Phys. Lett.* **70**, 3404 (1997); D. Andsager, J. Hilliard, J. M. Hetrick, L. H. AbuHassan, M. Plisch, and M. H. Nayfeh, *J. Appl. Phys.* **74**, 4783 (1993); Z. Yamani, S. Ashhab, A. Nayfeh and M. H. Nayfeh, *J. Appl. Phys.* **83**, 3929 (1998)
19. G. Belomoin, J. Therrien, and M. Nayfeh, *Appl. Phys. Lett.* **77**, 779, (2000); J. Therrien, G. Belomoin, and M. Nayfeh, *Appl. Phys. Lett.* **77**, 1668 (2000)
20. M. Nayfeh, N. Rigakis, and Z. Yamani, *Phys. Rev. B* **56**, 2079 (1997); *MRS* **486**, 243 (1998)